Electronic Supplementary Material (ESI) for Nanoscale.

Supporting Information

Tuning the Morphology and Chemical Distribution of Ag Atoms in Au rich Nanoparticles using Electrochemical Dealloying

Alexandra Dworzak[1,2], Paul Paciok[3], Christoph Mahr[4,5], Marc Heggen[3], Carsten Dosche[2], Andreas Rosenauer[4,5], Mehtap Oezaslan[1,2]*

[1]Technical Electrocatalysis Laboratory, Institute of Technical Chemistry, Technische Universität Braunschweig, Franz-Liszt-Str. 35a, 38106 Braunschweig, Germany.

[2]Institute of Chemistry, Carl von Ossietzky University of Oldenburg, Carl-von-Ossietzky-Str. 9-11, 26129 Oldenburg, Germany.

[3] Ernst Ruska-Center, Jülich Research Centre, 52425 Jülich, Germany.

[4]Institute of Solid State Physics, University of Bremen, Otto-Hahn-Allee 1, 28359 Bremen, Germany.

[5]MAPEX Center for Materials and Processes, University of Bremen, Bibliothekstr. 1, 28359 Bremen, Germany.

* Corresponding author: m.oezaslan@tu-braunschweig.de

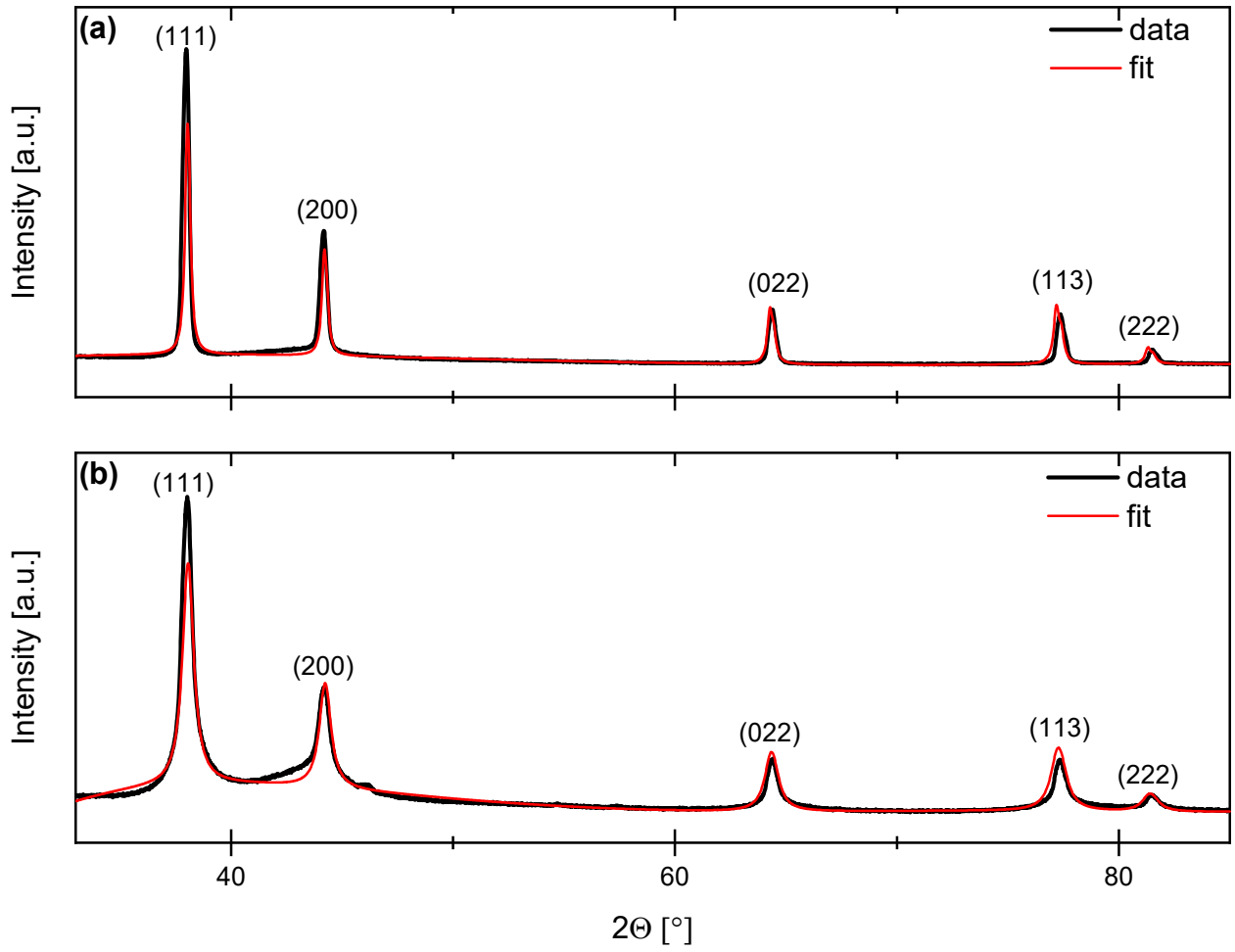

Figure S1. *XRD profiles and the respective calculated Rietveld refinement fits of Ag rich Ag-Au nanoparticles supported on carbon prepared by (a) wet-impregnation – freeze-drying – annealing and (b) one-pot synthetic routes. The Rietveld refinement was applied to determine the lattice parameter, quantification, and crystallite size of both as-prepared Ag rich NPs, listed in* ***Table S1****.*

***Table S1**. Results from the crystal structure including lattice parameter, Rietveld quantification, and crystallite size for the as-prepared Ag rich Ag-Au NPs. R_{wp} is the goodness of the fit. The crystallite size was determined by integral breadth method[1].*

Ag-Au NPs prepared by	**Lattice parameter [Å]**	**Rietveld quantification [wt.%]**	**Crystallite size [nm]**	**R_{wp}**
wet-impregnation – freeze-drying – annealing route	4.096 ± 0.001	100	27.9 ± 0.5	19.55
one-pot synthetic route	4.094 ± 0.001	100	10.4 ± 0.1	10.34

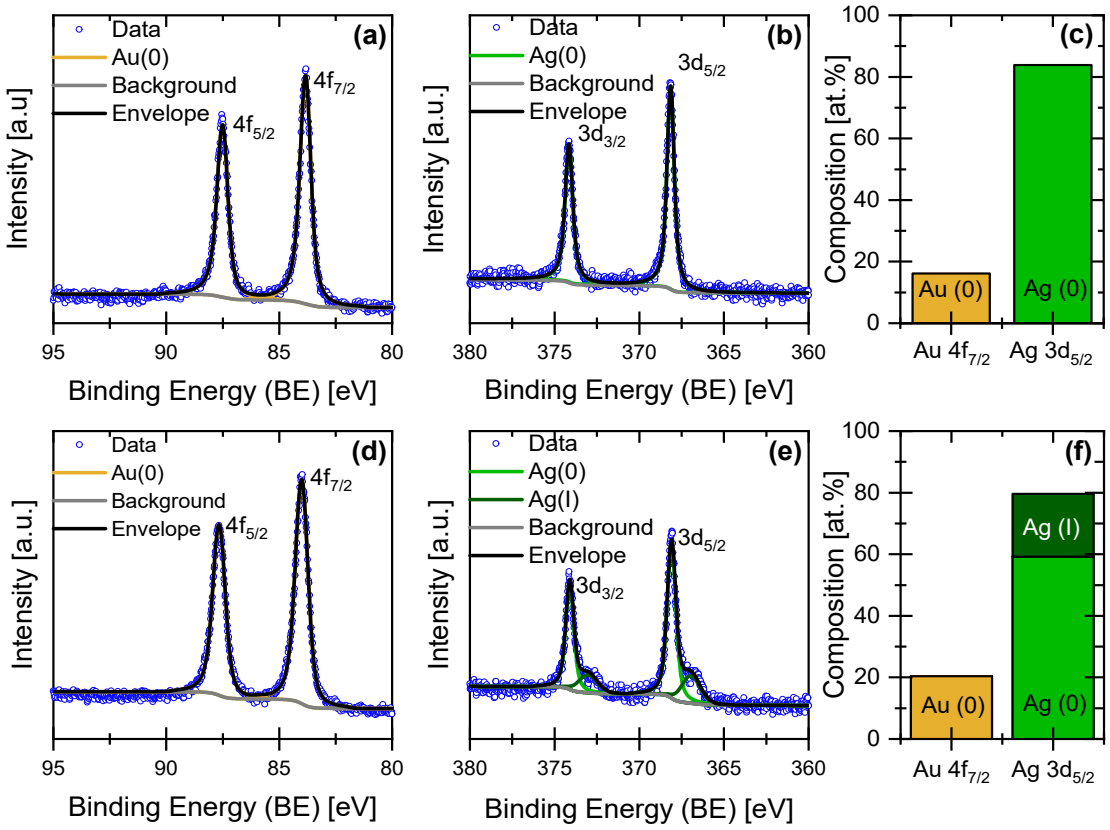

Figure S2. *High-resolution (a, d) Au 4f and (b, e) Ag 3d XPS spectra and the corresponding fits for the as-prepared (a, b) 77 nm $Ag_{77}Au_{23}$ and (d, e) 12 nm $Ag_{86}Au_{14}$ NPs. The XPS quantification shows 84 at.% Ag and 16 at.% Au for the (c) 77 nm $Ag_{77}Au_{23}$ NPs, while the (f) 12 nm $Ag_{86}Au_{14}$ NPs contain 20 at.% Au^0, 59 at.% Ag^0 and 21 at.% Ag^+. The EDX data also confirms the relative ratio of Ag and Au within the NPs obtained from the XPS data.*

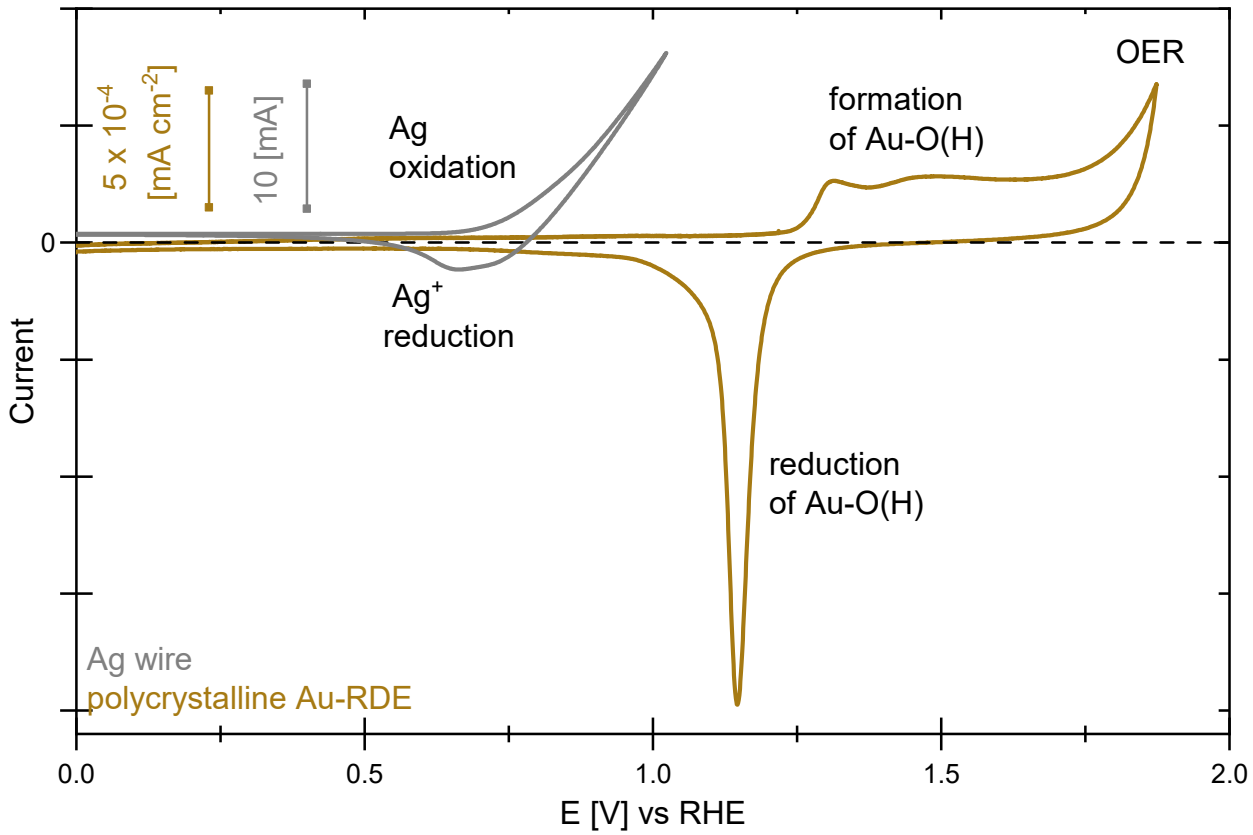

Figure S3. *Cyclic voltammetry (CV) profiles of polycrystalline Ag wire (silver grey) and Au disk (gold colored) recorded at scan rate of 20 mV* s^{-1} *in Ar-saturated 0.1 M* $HClO_4$*. For the polycrystalline Au, the current was normalized by the geometric surface area of the electrode disk, while the Ag wire did not have an exact electrode surface that had been immersed in the electrolyte. The y-axis is indicated with the respective scale bar of the current.*

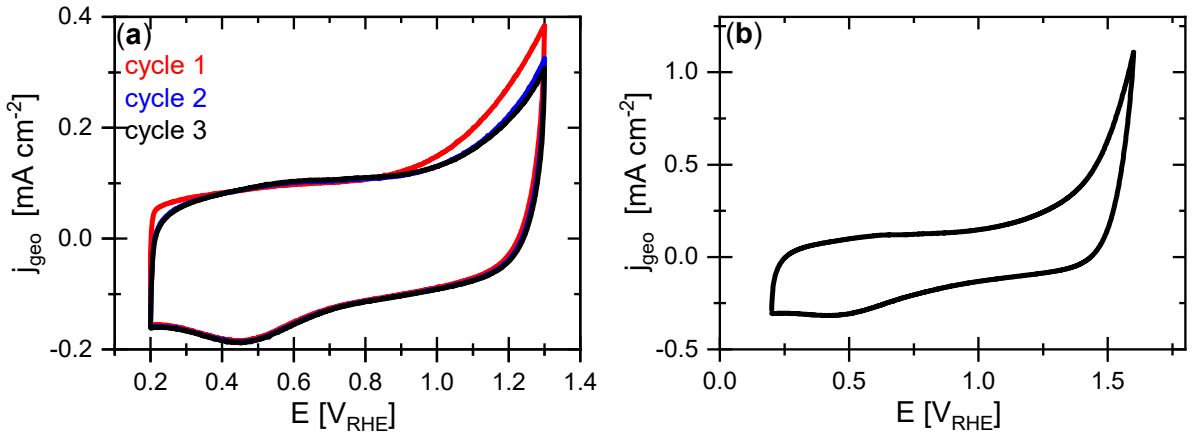

***Figure S4**. Initial cyclic voltammetry (CV) profiles of Vulcan XC72, showing the carbon corrosion behavior between (a) 0.2 – 1.3 V_{RHE} and (b) 0.2 – 1.6 V_{RHE} at 20 mV s^{-1} and 1600 rpm in Ar-saturated 0.1 M $HClO_4$. The carbon loading was ~7 µg cm^{-2}.*

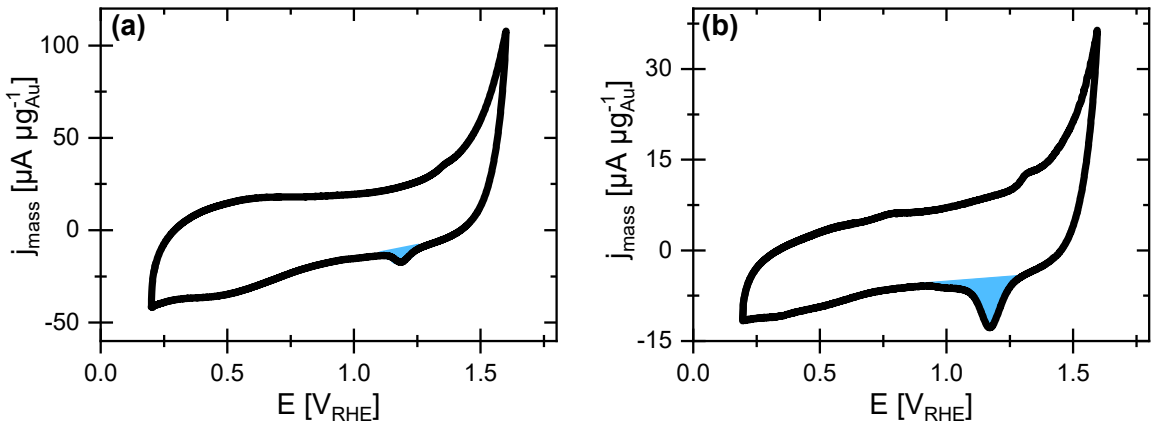

Figure S5. *Cyclic voltammetry profiles of (a) 77 ± 26 nm $Ag_{77}Au_{23}$ NPs and (b) 12 ± 5 nm $Ag_{86}Au_{14}$ NPs after dealloying to probe the Au-OH region in Ar-saturated 0.1 M $HClO_4$. Experimental parameters: 0.2 – 1.6 V_{RHE}, 1600 rpm, 20 mV s^{-1}, Pt wire and MMS as counter and reference electrodes, respectively. The turquoise filled region denotes the reduction current peak of Au-O monolayer between 1.1 – 1.2 V_{RHE}, while the high current peak at the upper vertex potential is mainly based on the carbon corrosion (compare with* ***Figure S4****).*

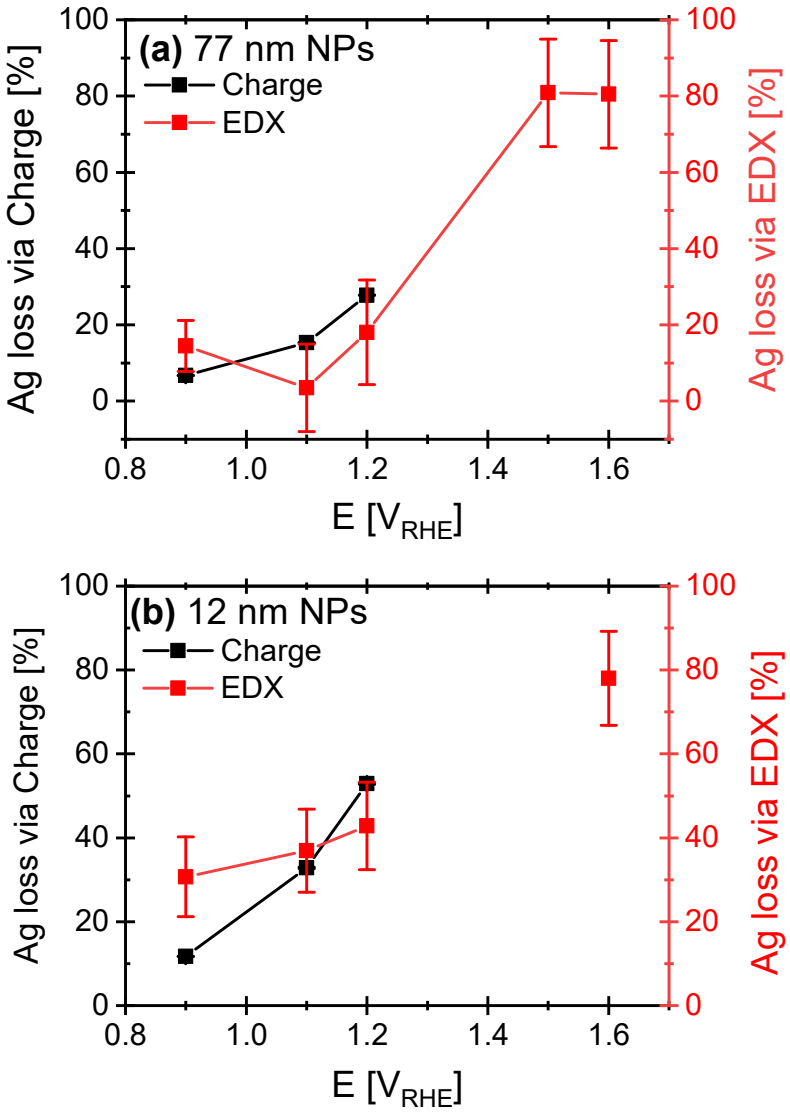

Figure S6. *Comparison of the Ag losses for the (a) 77 nm $Ag_{77}Au_{23}$ NPs and (b) 12 nm (b) $Ag_{86}Au_{14}$ NPs after potentiostatic dealloying by holding at different potentials for 15 minutes in Ar-saturated 0.1 M $HClO_4$. The Ag dissolution was either determined from the EDX data (in red, shown in Tables S2) or from the electric charge (in black) using Faraday's law. Above 1.2 V_{RHE}, the carbon corrosion dominates and therefore the electric charge is not reliable to detect only the Ag dissolution process. The low Ag loss determined from EDX in (a) at 1.1 V_{RHE} relative to those at higher anodic potentials is very likely due to the low statistical analysis of the single particle STEM-EDX data. However, the corresponding charge indicates an overall Ag loss in dependence of the potential applied.*

Table *S2.* *Comparison of the Ag content for two size groups of Ag rich Ag-Au master nanoparticles (NPs) after potentiostatic and potentiodynamic dealloying conditions in Ar-saturated 0.1 M $HClO_4$ at room temperature. The Ag content was determined from SEM-EDX for the as-prepared master alloy NPs, while the STEM-EDX measurements were applied to evaluate single nanoparticles after potentiostatic dealloying.*

	Ag content [at.%] determined via EDX	
	77 ± 26 nm NPs	**12 ± 5 nm NPs**
master alloy	77 ± 3 at.%	86 ± 2 at.%
potentiostatic dealloying via CA method		
at 0.9 V_{RHE}	66 ± 3 at.%	60 ± 7 at.%
at 1.2 V_{RHE}	63 ± 10 at.%	49 ± 8 at.%
at 1.6 V_{RHE}	15 ± 8 at.%	19 ± 8 at.%
Potentiodynamic dealloying via CV method		
0.2 – 1.3 V_{RHE}	14 ± 9 at.%	17 ± 8 at.%

Table S3. *Absolute and relative Ag losses for both size groups determined from the EDX measurements of Ag rich Ag-Au master nanoparticles (NPs) after potentiostic and potentiodynamic dealloying conditions in Ar-saturated 0.1 M $HClO_4$ at room temperature. The absolute Ag loss was calculated from the initial composition of 77 nm $Ag_{77}Au_{23}$ and 12 nm $Ag_{86}Au_{14}$ master NPs, while the relative loss is the percentage of the absolute loss from the initial composition.*

	77 ± 26 nm NPs		**12 ± 5 nm NPs**	
	absolute loss	relative loss	absolute loss	relative loss
potentiostatic dealloying via CA method				
at 0.9 V_{RHE}	11 ± 6 at.%	14 ± 7 %	26 ± 9 at.%	31 ± 9 %
at 1.2 V_{RHE}	14 ± 13 at.%	18 ± 14 %	37 ± 10 at.%	43 ± 10 %
at 1.6 V_{RHE}	62 ± 11 at.%	80 ± 14 %	67 ± 10 at.%	78 ± 11 %
potentiodynamic dealloying via CV method				
0.2 – 1.3 V_{RHE}	63 ± 12 at.%	82 ± 15 %	69 ± 10 at.%	80 ± 11 %

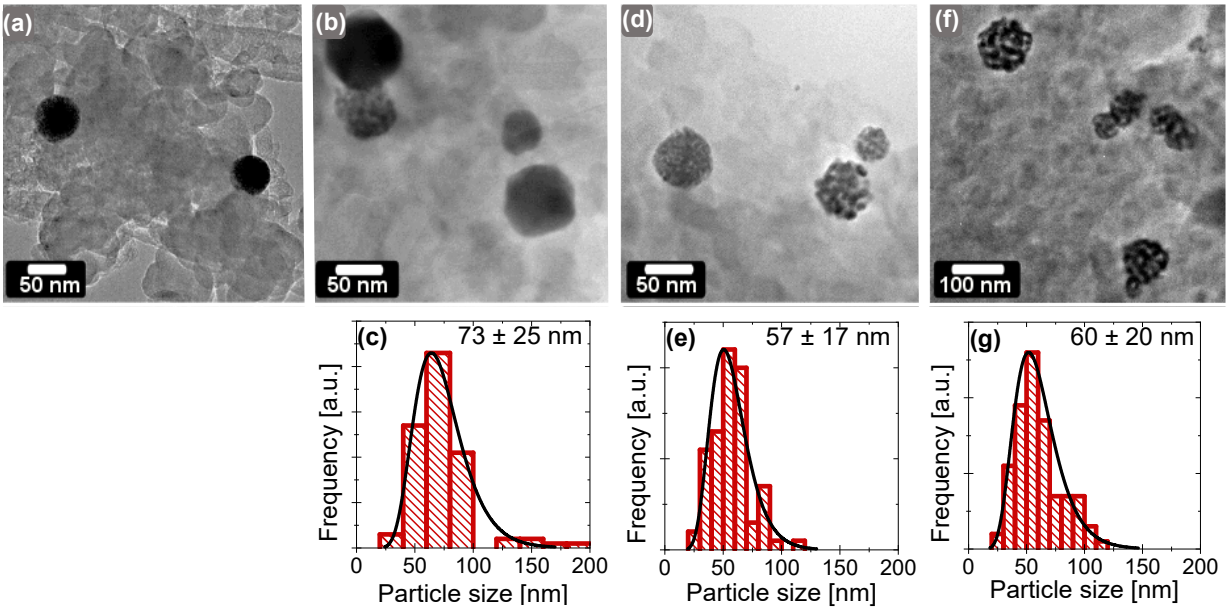

Figure S7. *(top) TEM micrographs and (bottom) corresponding particle size distributions of initial 77 ± 26 nm $Ag_{77}Au_{23}$ NPs dealloyed after potentiostatic method at (a) 0.9 V_{RHE}, (b, c) 1.2 V_{RHE}, and (d, e) 1.6 V_{RHE} for 15 minutes as well as after (f, g) potentiodynamic method (0.2 – 1.3 V_{RHE} at 20 mV s^{-1} and 16 cycle numbers).*

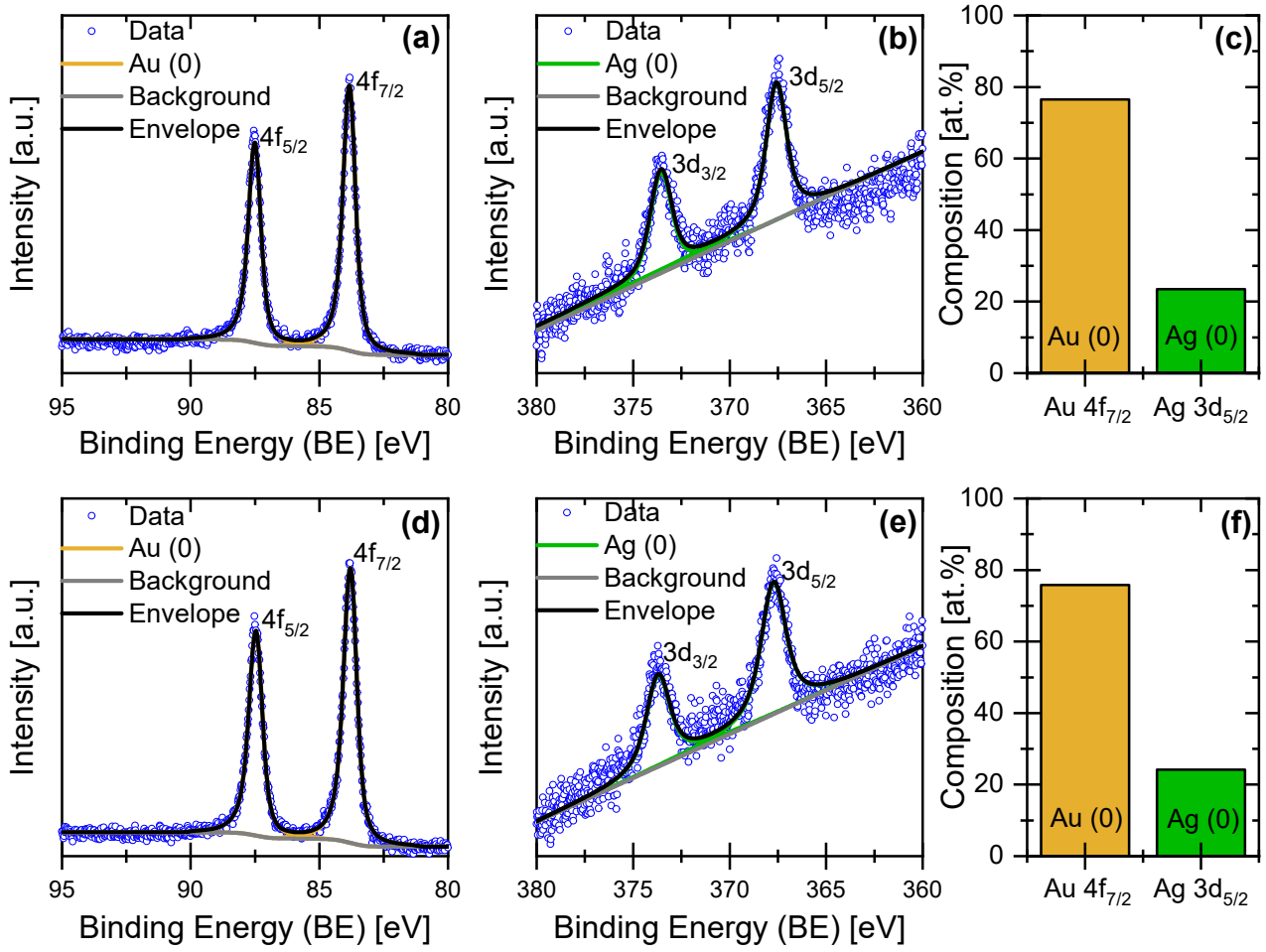

***Figure S8**. High-resolution (a, d) Au 4f and (b, e) Ag 3d XPS profiles and the corresponding fits for the 77 nm $Au_{77}Ag_{23}$ after (a, b) potentiodynamic and (d, e) potentiostatic (at 1.6 V_{RHE}) dealloying experiments. (c, f) The XPS quantification yielded 24 at.% Ag and 76 at.% Au irrespective of the dealloying protocol.*

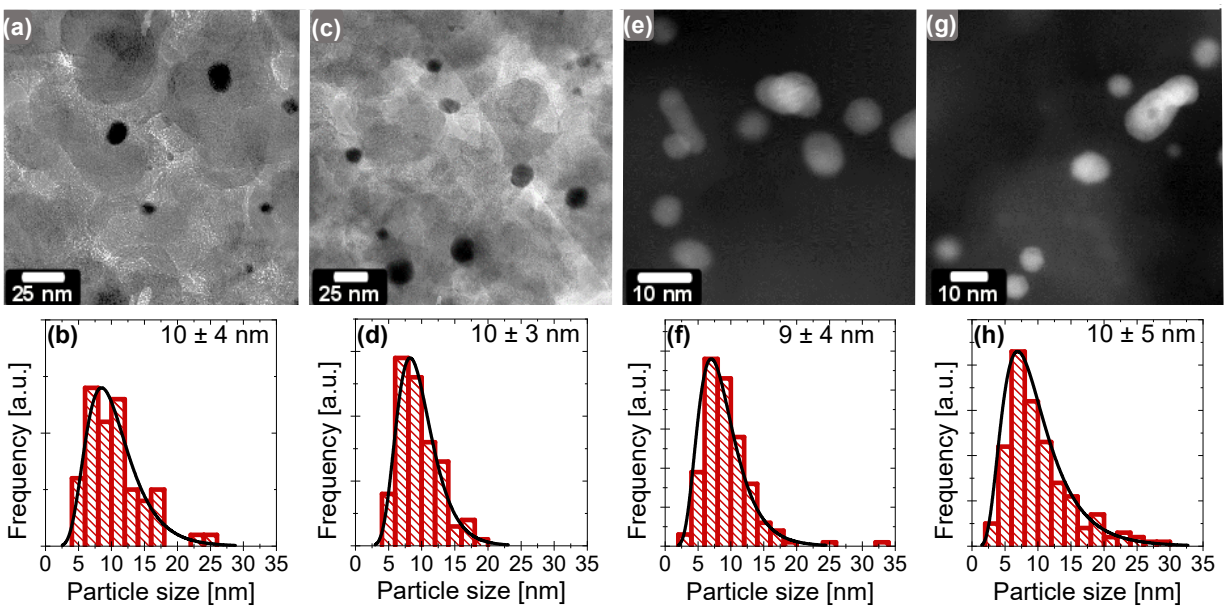

***Figure S9**. (a, c) TEM and (e, g) HAADF-STEM micrographs and (b, d, f, h) corresponding particle size distributions of the initial 12 ± 5 nm $Ag_{86}Au_{14}$ NPs dealloyed after potentiostatic method at (a, b) 0.9 V_{RHE}, (c, d) 1.2 V_{RHE}, and (e, f) 1.6 V_{RHE} for 15 minutes as well as after (g, h) potentiodynamic method (0.2 – 1.3 V_{RHE} at 20 mV s^{-1} and 16 cycle numbers).*

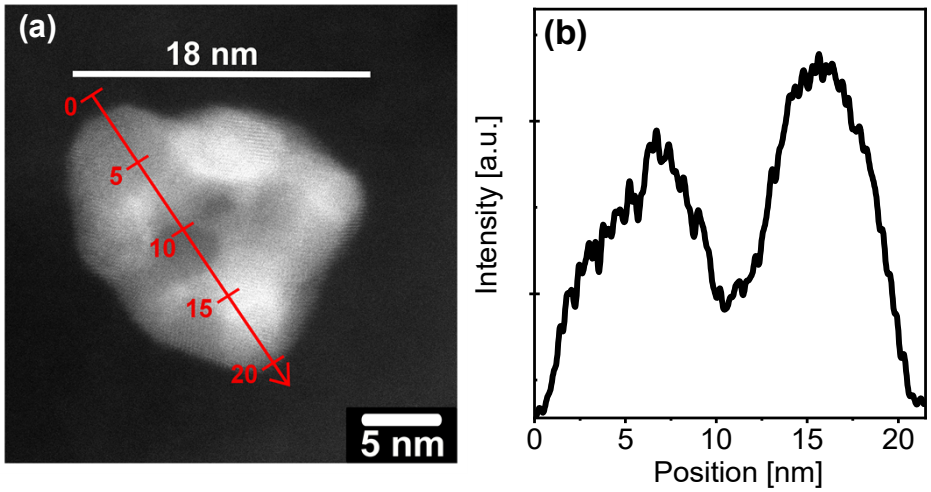

Figure S10. *(a) HAADF-STEM image and (b) corresponding line scan of the image intensity of a single Au rich NP after potentiodynamic dealloying in Ar-saturated 0.1 M* $HClO_4$*. This dealloyed NP is among the smallest porous NP observed in this work.*

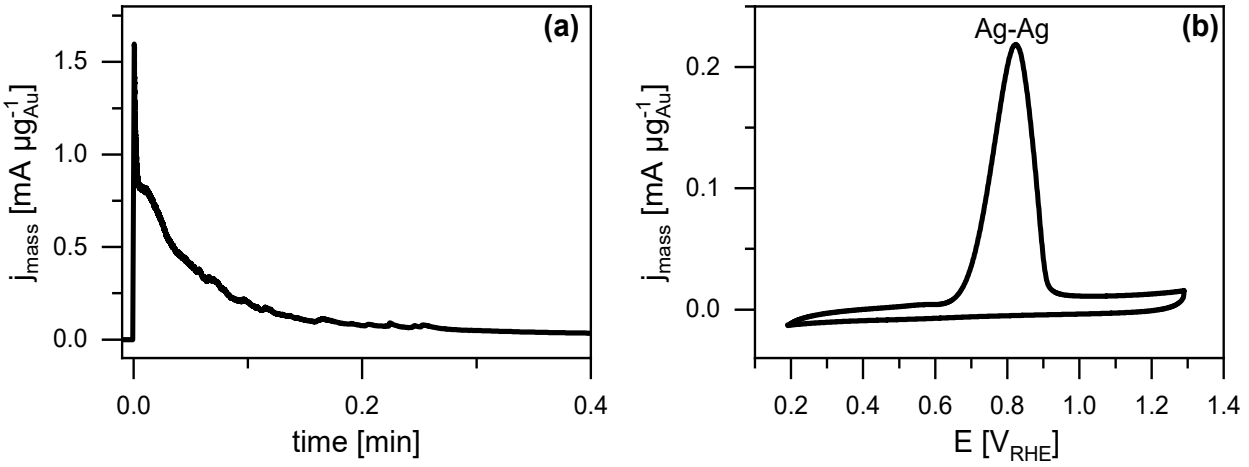

Figure S11. *(a) Chronoamperometric dealloying profile of the initial 12 ± 5 nm* $Ag_{86}Au_{14}$ *master NPs at 1.6* V_{RHE} *for 15 min. followed by (b) first cyclic voltammetry profile between 0.2 – 1.3* V_{RHE} *at 20 mV* s^{-1} *in fresh Ar-saturated 0.1 M* $HClO_4$*. The current was normalized by the geometrical surface area.*

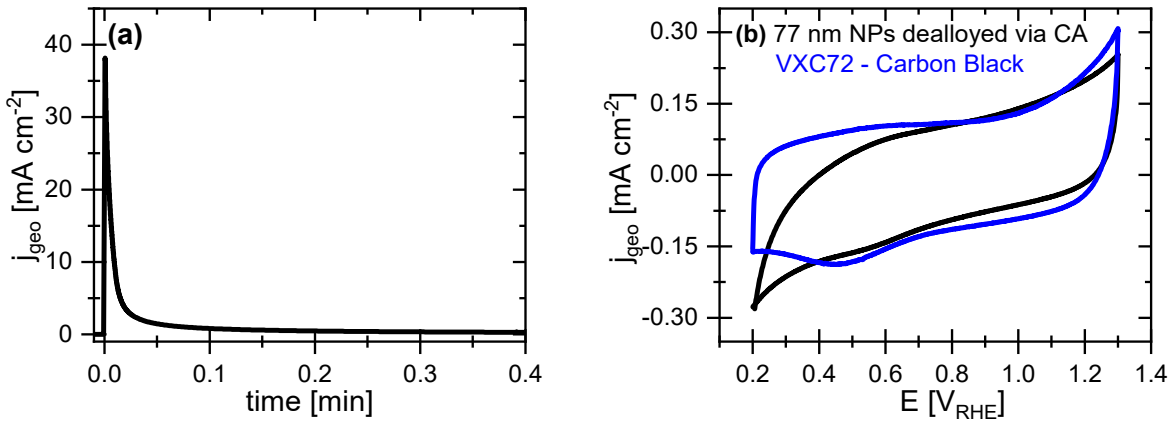

Figure S12. *(a) Chronoamperometric dealloying profile of the initial 77 ± 26 nm $Ag_{77}Au_{23}$ master NPs at 1.6 V_{RHE} for 15 min. followed by (b) first cyclic voltammetry profile between 0.2 – 1.3 V_{RHE} at 20 mV s^{-1} in fresh Ar-saturated 0.1 M $HClO_4$. (b) CV profile of the VXC72 carbon black denoted in blue line. The current was normalized by the geometrical surface area.*

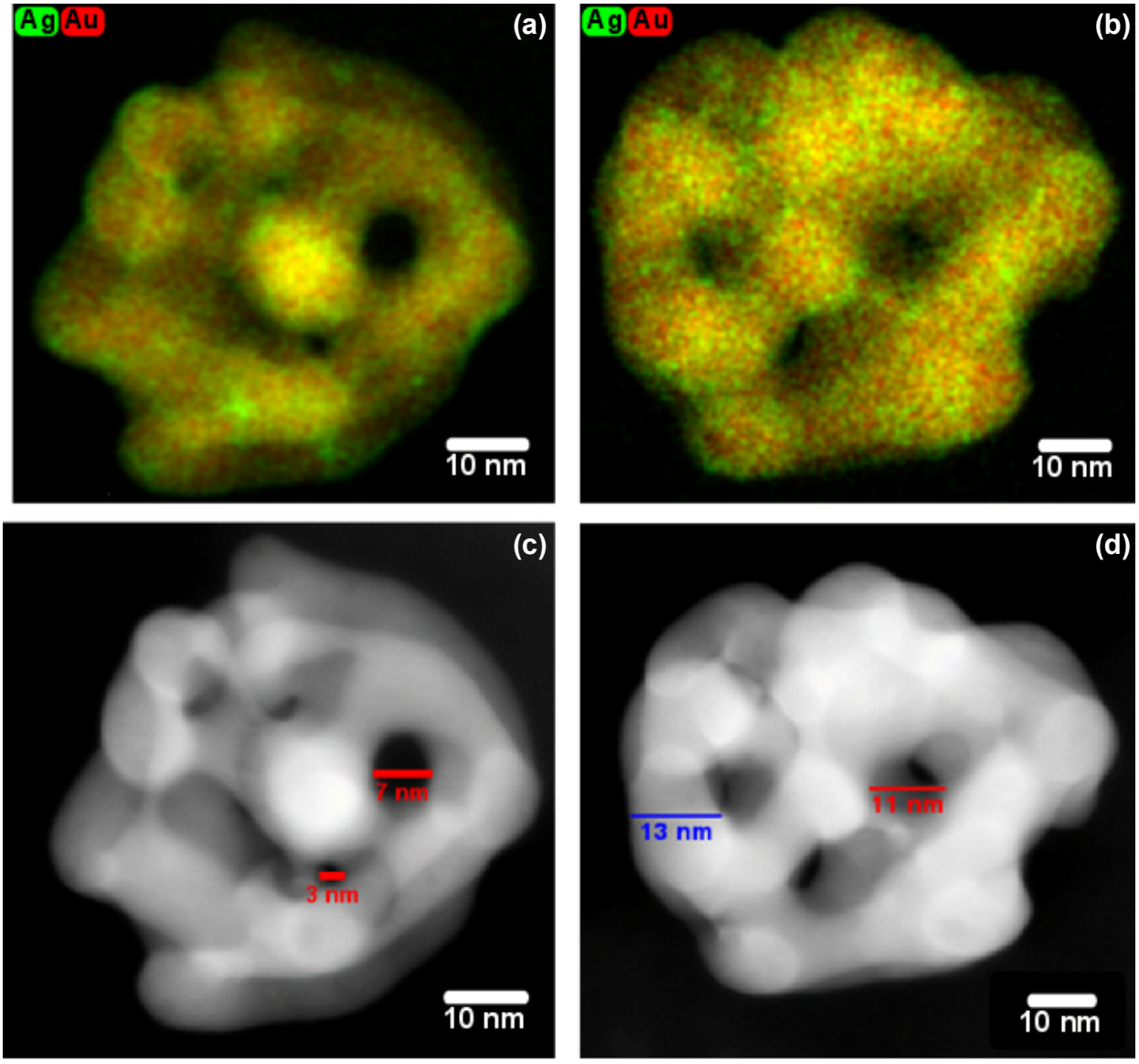

Figure S13. *(a, b) Overlaid EDX maps and (c, d) HAADF-STEM images of the initial 77 ± 26 nm* $Ag_{77}Au_{23}$ *NPs dealloyed under (a, c) potentiostatic at 1.6* V_{RHE} *for 15 minutes and (b, d) potentiodynamic (*0.2 – 1.3 V_{RHE} at 20 mV s^{-1} and 16 cycle numbers) *conditions.*

References

(1) Laue, M. v. VI. Lorentz-Faktor und Intensitätsverteilung in Debye-Scherrer-Ringen. *Zeitschrift für Kristallographie - Crystalline Materials* **1926**, *64* (1-6), 115–142. DOI: 10.1524/zkri.1926.64.1.115.